The geochemistry and petrogenesis of the Paleoproterozoic du Chef dyke swarm, Québec, Canada

T. Jake. R. Ciborowski*[1], Andrew C. Kerr[1], Iain McDonald[1], Richard E. Ernst[2], Hannah S. R. Hughes[1], and Matthew J. Minifie[1].

[1]School of Earth and Ocean Sciences, Cardiff University, Park Place, Cardiff, Wales, CF10 3AT, UK

[2]Department of Earth Sciences, Carleton University, 1125 Colonel By Drive, Ottawa, Ontario, K1S 5B6, Canada & Ernst Geosciences, 43 Margrave Ave. Ottawa, Ontario K1T 3Y2, Canada

*email: jake.ciborowski@live.co.uk Telephone: +44 (0) 2920 876420

Abstract

The du Chef dyke swarm in southern Québec, Canada is composed of numerous northeast trending, greenschist-amphibolite facies, gabbronoritic dykes that crop out either side of the Grenville Front. The age of the du Chef swarm (2408±3 Ga) has led previous authors to suggest a genetic link between the du Chef dykes and coeval swarms (including the Ringvassøy, Scourie, Widgemooltha and Sebanga) preserved on other Archean cratons. These now disparate dyke swarms are proposed to have formed in response to mantle plume-induced continental breakup during the early Proterozoic. This work represents the first geochemical study of the du Chef dykes and shows that the swarm evolved through fractional crystallisation of a tholeiitic parent magma that remained largely uncontaminated during its residence in, and ascent through, the crust. We also show that the primary magma for the du Chef swarm was derived through partial melting of an enriched region of the mantle, with a similar trace element composition to the modern-day HIMU reservoir and that the magma produced was significantly hotter than the ambient mantle at the time. We contend that the du Chef dykes are the product of early Proterozoic mantle plume magmatism and may help pinpoint an ancient hotspot centre that initiated continental break up along the margin of the

Superior Craton at ~2.4 Ga. Other dyke swarms proposed to be genetically linked with the du Chef dykes record a distinctly different petrogenetic history to that of the du Chef dykes, as evidenced by their more volcanic arc-like geochemical signature. These contrasting geochemical signatures in supposedly cogenetic continental tholeiitic rocks may be evidence of early Proterozoic mantle heterogeneity sampled by the rising du Chef mantle plume.

1. Introduction

The du Chef dykes were first described by Ciesielski and Madore (1989) as a series of north-north east trending discordant intrusions which have a maximum thickness of 30 metres and a measurable strike length of up to several kilometres. The majority of the dykes crop out within the Grenville Province and have been amphibolitised and otherwise deformed by Grenvillian tectonism such that the igneous mineralogy is rarely preserved, being more commonly altered to garnet, amphibole, plagioclase, epidote and sphene (Ciesielski and Madore 1989). Krogh (1994) reports the only published age of the du Chef dykes and interprets the dykes to have been emplaced at 2408±3 Ma. This age is based on U-Pb analysis of two samples of magmatic zircons from a pegmatitic portion of a ~ 40 m wide amphibolitised du Chef dyke that was also sampled (DC007) during this study.

Several workers have noted that the age of the du Chef dykes, and other swarms that intrude the Superior Craton, overlap with those of dyke swarms preserved on the North Atlantic, Karelia, Zimbabwe and Yilgarn cratons (Ernst and Buchan 2002; Kulikov et al. 2010; Pirajno and Hoatson 2012). This coeval magmatism has been argued to represent the remnants of an early Proterozoic Large Igneous Province (LIP) that formed during mantle plume-driven breakup of an Archean supercontinent (Ernst and Buchan 2004; Söderlund et al. 2010).

This work presents the first whole-rock major and trace element data for du Chef dykes from either side of the Grenville Front. These data are used to characterise the petrogenetic evolution of the swarm, investigate potential mantle sources of the primary magmas, evaluate the proposed mantle plume origins of the swarm and investigate potential genetic links with other coeval swarms preserved on other Archean cratons.

2. Regional Geology

The Superior Craton is the largest of the Archean cratons and forms the core of the Canadian Shield. It is composed of alternating, east-west trending granite-greenstone and

metasedimentary terranes which are commonly in fault-bounded contact with each other. The granite-greenstones and intervening metasediments are widely considered to represent ancient volcanic arcs and accretionary prisms that were sutured and cratonised during the late Archean (e.g., Card 1990; Stachel et al. 2006). Superior Craton terranes which share a common tectonic history are grouped into a number of provinces, the largest being the Superior Province. On its eastern margin, the Superior Province is in fault-bounded contact with the Grenville Province, the latter being interpreted to be the eroded remnants of a Himalayan-style continental orogen caused by the collision of Baltica and Laurentia during the middle Proterozoic (Dufrechou and Harris 2013).

Near Chibougamau **(Fig. 1)**, the Archean basement of Superior Province to the west of the Grenville Front is composed of; greenschist-facies bimodal volcanic rocks, banded iron formations, cherts, conglomerates, sandstones, argillites and alkalic-shoshonitic volcanic rocks (Leclerc et al. 2011). These rocks are intruded by the ~2.73 Ga anorthositic Lac Dorè complex (and other) tonalitic intrusions; and all are unconformably overlain by Proterozoic metasediments and bimodal volcanics of the Huronian Supergroup (Card 1990). Close to the margin of the Superior Province, the east-west trending lithotectonic boundaries of the Archean groups are deflected to the northeast before being truncated at the Grenville Front. Immediately east of the Grenville Front, the dominant lithotectonic trends are orientated northeast-southwest (parallel to the Grenville Front) and metamorphic grade reaches amphibolite-granulite facies (Ciesielski and Madore 1989; Martignole and Martelat 2005).

3. Sample collection and petrography

Given the low topographic relief and dense vegetation of southwest Québec, sample collection **(Fig. 1)** was limited to road cuts along Highway 167 and adjoining logging roads **(Supplementary Figure 1A)** as well as a few isolated whale-back type exposures **(Supplementary Figure 1B)**. In outcrop, the du Chef dykes are dark green-black in colour and range in thickness from 1-2 m, up to 40 m. The dykes are steeply dipping and generally trend northeast-southwest. Aside from these features shared by all du Chef dykes, stark differences in appearance are observed between dykes from areas northwest of the Grenville Front to those preserved within the Front. The most readily observed difference is the nature of the dyke margins, in that the dykes from outside of the Grenville Front typically preserve very sharp and regular contacts with the country rock **(Supplementary Figure 1C)** while in contrast, the margins of du Chef dykes from within the Grenville Front are more irregular

with the dykes appearing to finger into the country rock **(Supplementary Figure 1D)**. Amphibolitised du Chef dykes from within the Grenville Front also commonly preserve a foliated fabric and have mineralogies characterised by occasionally abundant garnet **(Supplementary Figure 1E)**, while those from outside of the Grenville Front preserve igneous textures, particularly in the coarser interiors of thicker dykes **(Supplementary Figure 1F)**.

The amphibolitised du Chef dykes are generally equigranular and fine grained **(Fig. 2A)**. Amphibole dominates the mineralogy of the studied samples and shows a range of crystal habits from euhedral, equant prisms to anhedral, irregular forms which commonly contain very fine inclusions of quartz. The next most abundant mineral is plagioclase which forms irregularly shaped crystals with well-developed twins that appear to fill the spaces between the amphibole crystals. A planar foliation is commonly observed in the amphibolitised du Chef dykes caused by alignment of amphibole and plagioclase crystals into alternating bands **(Fig. 2B)**.

Accessory phases within such amphibolitised samples include biotite which tends to form elongated lath shaped crystals intergrown with the amphibole, and both pyrite and magnetite which form euhedral crystals or glomerocrysts distributed throughout the rock **(Fig. 2C)**. In some samples, porphyroblasts of garnet are preserved as medium grained, euhedral crystals distributed throughout the rock **(Figs. 2D and 2E)**. Occasionally, the interiors of the garnets are filled with fine grained inclusions of plagioclase, amphibole, biotite, and chlorite and often, the garnets display atoll textures **(Fig. 2F)**.

In less metamorphosed samples, from northwest of the Grenville Front, primary igneous minerals and textures are partially preserved. Typically, the interiors of these dykes are medium grained and inequigranular **(Fig. 2G)**. The most abundant primary phase is olivine, which forms euhedral relict grains that have been altered to magnesite, serpentine and iron oxides, predominantly along grain boundaries and crystal fractures. Plagioclase tends to form very elongate laths which appear to be overgrown by the olivine crystals. Alteration of the plagioclase is characterised by very fine grained quartz and sericite concentrated along crystal margins **(Fig. 2H)**. Very little primary pyroxene remains in the studied samples, but its original existence is confirmed by pseudomorphic replacements by calcite and amphibole.

In summary, the du Chef dykes record metamorphic mineral assemblages which range from lower greenschist to upper amphibolite facies. The transition from greenschist to amphibolite facies parallels the trend of the Grenville Front in this region **(Fig. 1)**. The extent to which this metamorphism has affected the geochemistry of the dykes is explored in the subsequent sections.

4. Geochemistry

4.1 Analytical procedures

Sample preparation and analysis was carried out at Cardiff University. Weathered surfaces and veins were removed with a rock saw prior to analysis. The sawed samples were crushed into ~5 mm chips using a steel jaw crusher and powdered in an agate planetary ball mill. Approximately 2 g of the milled powder was ignited in a furnace at 900 °C for two hours in order to determine loss on ignition values.

Whole-rock major element, trace element and rare earth element (REE) data were obtained following Li metaborate fusion (Minifie et al. 2013). Major element and Sc abundances were determined using a JY Horiba Ultima 2 Inductively Coupled Plasma Optical Emission Spectrometer (ICP-OES). Trace elements were analysed by a Thermo X Series 2 Inductively Coupled Plasma Mass Spectrometer (ICP-MS). International reference material JB-1A was run with each sample batch to constrain the accuracy and precision of the analyses. Relative standard deviations show precision of 1–5% for most major and trace elements for JB-1A. 2σ values encompass certified values for the vast majority of elements. Full analytical results including repeat runs of standard basalt JB-1A can be found in the Supplementary Information. Representative, whole-rock major element and trace element data for the du Chef dyke samples are presented in **Table 1**.

4.2 Element mobility

As the du Chef dyke swarm crops out within the Grenville Province where metamorphic facies extends to amphibolite-granulite facies (Martignole and Martelat 2005) and samples show abundant alteration **(Fig. 2)**, the effects of secondary element remobilisation must be considered. At metamorphic conditions above lower amphibolite facies the normally immobile high field strength elements (HFSE) including the REE are expected to become more mobile (Pearce 1996) and therefore any scatter observed in plots involving these elements for the du Chef samples may reflect their metamorphic history. As the HFSE are

incompatible in the main rock forming minerals, they should plot on linear arrays when plotted against each other for a suite of unaltered rocks formed from a common fractionating magma, whereas secondary remobilisation of elements is likely to result in a scattered trend (Cann 1970).

Good linear correlations are observed between Zr and the REE and other HFSE ($R^2 \geq 0.7$), indicating that secondary remobilisation of these elements was very limited. Conversely, the incompatible large ion lithophile elements (LILE) show much more scattered correlations with Zr which indicates that these elements have undergone sub-solidus remobilisation. A subset of these graphs is shown in **Figure 3**. The following petrogenetic discussion will largely be limited to use of the HFSE which are likely to record near-primary concentrations.

4.3 Major elements

The du Chef dykes are broadly basaltic in major element composition **(Table 1)** with, MgO ranging from 5.4 to 9.0 wt.% and are relatively TiO_2 poor (1.0 to 2.7 wt.%). Na_2O, K_2O, TiO_2, and MnO do not show any obvious correlation with MgO while SiO_2, Al_2O_3, and CaO have positive, and P_2O_5 negative, correlations with MgO **(Supplementary Figure 2)**. Fe_2O_3 shows an enrichment trend characteristic of tholeiitic magmas. The poor correlations observed between MgO and the alkalis are further evidence of element mobility in the du Chef dykes while the better correlations observed between MgO and Fe_2O_3, SiO_2, Al_2O_3, and CaO may suggest that the dykes evolved through the fractional crystallisation and removal of olivine, clinopyroxene and plagioclase from a tholeiitic parent magma.

4.4 Trace elements

The du Chef dykes have relatively low concentrations of Cr and Ni **(Fig. 4)** which show positive correlations with MgO. Other compatible trace elements including Sc and V have more scattered but negative correlations with MgO. Those trace elements which are incompatible during basaltic fractionation show slightly scattered negative correlations with MgO. On similar graphs where relatively immobile Zr **(Fig. 3)** is used instead of MgO as an index of fractionation, the incompatible elements plot on much tighter, positively correlated arrays suggesting that the du Chef dykes may have formed by the fractionation of parent magmas of similar composition.

Total rare earth element (REE) abundances in the du Chef dykes range between 15 – 49 × chondritic values and when plotted on chondrite-normalised REE diagrams **(Fig. 5)**, the dykes show sub-parallel trends enriched in light REE [$(La/Sm)_N = 1.9 \pm 0.3$] relative to the HREE which themselves are characterised by $(Gd/Yb)_N$ ratios of 1.31 ± 0.26. Variable but slightly positive Eu anomalies may indicate the presence of cumulate plagioclase in the magma. The enrichment of the light REE relative to the heavy REE increases with fractionation **(Supplementary Figure 3)** while the magnitude and direction of the Eu anomaly does not change.

4.5 Classification

The total alkali silica diagram is a common way to geochemically classify igneous rocks, however since Na and K have been remobilised in the du Chef dykes, the total alkali silica diagram cannot be used. Instead, we use the Zr/Ti vs. Nb/Y diagram **(Fig. 6)** since the elements used in this classification have been shown to have remained immobile. On this diagram, the du Chef dykes plot as a fairly tight cluster within the subalkaline basalt and basaltic andesite fields.

5. Modelling and discussion

5.1 Fractional crystallisation

The linear geochemical trends exhibited by the du Chef dykes suggest that the dykes evolved by the fractionation of parental magmas of similar composition. In this section, we will evaluate fractional crystallisation as a potential mechanism for generating the geochemical trends observed in the du Chef dykes. Fractional crystallisation of the most primitive du Chef dyke sample (DC011) has been modelled using the PELE computer software program (Boudreau 1999). This sample is unlikely to be a primary magma given its relatively evolved nature (~ 9 wt.% MgO), however, it represents the most primitive magma of the suite and hence, the closest estimate of the primary magma for the suite.

PELE is a Windows®-compatible computer program which allows the user to evaluate crystallisation of silicate magma at varying physical conditions. Boudreau (1999) used published descriptions of the database and numerical models used by the MELTS (Ghiorso & Sack 1995) software (currently usable as a JAVA® enabled web applet from http://melts.ofm-research.org/applet.html) to produce a modified version of the program for use with Windows® systems (PELE). For a detailed description of the workings of PELE, the

reader is referred to Ghiorso & Sack (1995), Asimow and Ghiorso (1998) and Boudreau (1999). The major element geochemical trends for the du Chef dykes have been modelled using six different scenarios of varying pressure and water content **(Table 2)**. All models use a quartz-fayalite-magnetite (QFM) oxygen buffer and calculate the composition of the liquid at 10% crystallisation intervals.

It is not entirely obvious which model best approximates the major element composition of the du Chef dykes, partly due to the scatter resulting from sub-solidus element mobility, but also because for certain elements (e.g., CaO and P_2O_5), the models predict similar trends **(Fig. 7)**. However, high-pressure fractional crystallisation of the du Chef dyke parent magmas is supported by the TiO_2, SiO_2, Al_2O_3 and Fe_2O_3 compositions, the trends of which (when plotted against MgO) are best approximated by models 5 (7 kbar) and 6 (10 kbar). Overall, model 5, which models fractional crystallisation of a magma with a composition equal to that of sample DC011 at 7 kbar, provides the most consistent fit with the du Chef dyke compositions.

The 7 kbar model predicts that crystallisation of the DC011 parent magmas begins at ~1261 °C with olivine being the first mineral to crystallise. Clinopyroxene joins olivine at ~1249 °C after ~3% of the magma has crystallised. Clinopyroxene is followed by plagioclase soon after at 1242 °C after ~6% of the magma has crystallised. Once the magma has cooled to 1212 °C and ~44% of it has crystallised, orthopyroxene joins the crystallising assemblage before leaving again once the magma cools to 1170 °C and ~65% of it has crystallised. Olivine, clinopyroxene and plagioclase continue to crystallise until the magma reaches 1160 °C, at which point 70% of the original parent magma has crystallised and the remaining liquid contains less MgO than the most evolved du Chef dyke sampled **(Fig. 8)**.

5.2 Crustal contamination

On primitive mantle-normalised multi-element diagrams **(Fig. 9)**, the du Chef dykes show similar subparallel trends to those observed on chondrite normalised REE diagrams **(Fig. 5)**. All of the du Chef samples show enrichments in the most incompatible elements relative to the more compatible HFSE and have relative depletions in Th [$(Th/La)_N = 0.37 \pm 0.18$]. The dykes also show negative Nb anomalies ($Nb_N/Nb_N^* = 0.8 \pm 0.2$)[1] and variable Ti anomalies

[1] $Nb_N^* = (Th_N + La_N) / 2$

($Ti_N/Ti_N^* = 1.1 \pm 0.5$)[2] the magnitude of which do not correlate with degree of fractionation **(Supplementary Figure 3)**. The du Chef dykes are further characterised by predominantly negative Zr-Hf anomalies. These trace element characteristics result in the majority of the du Chef dykes plotting in mantle plume-related oceanic plateau basalt fields on the Nb/Y vs. Zr/Y and Zr/Nb vs. Nb/Th diagrams **(Fig. 10)**.

Trace element models have been constructed to determine whether the du Chef parental magma evolved via simple fractional crystallisation (FC) or through assimilation-fractional crystallisation (AFC). Fractional crystallisation of the du Chef parent magma was modelled using the modal mineral abundances predicted by the 7 kbar major element model and the partition coefficients of Bedard (2001) using **equation 1 (see supplementary information)**. AFC uses the same parameters as the FC model, the composition of felsic crust (Rudnick and Gao 2003) and an assimilation/fractionation rate (r) of 0.1 (**equations 2** and **3)**.

Models which use trace elements to model FC and AFC using the parameters and assemblages predicted at various degrees of crystallisation at 7 kbar are shown in **Fig. 9**. Both FC and AFC models predict the general trends of increasing incompatible element abundances observed in the du Chef dykes. However, the AFC model indicates that as fractionation of the parent magma continues, the magmas develop an increasingly negative Nb-Ta anomaly. The lack of correlation between Nb_N/Nb_N^* and Zr or MgO (used as an index of fractionation) in the du Chef dykes **(Supplementary Figure 3)** shows that contamination of the fractionating du Chef parent magma by felsic crust is unlikely. Instead, fractionation of the du Chef dyke parent magma, with no significant input of crustal material is our preferred mechanism for explaining the trace element variation observed in the dykes. However, despite the lack of systematic change in the dykes' Nb_N/Nb_N^* values, some of the scatter on **Supplementary Figure 3** may be the product of in situ contamination of individual dykes by heterogeneous lithologies which make up the ~10,000 km^2 area within the Grenville Province (Martignole and Martelat 2005) that the du Chef dykes crop out in **(Fig. 1)**.

In summary, the major element chemistry of the du Chef dykes is best explained by a model that involves basaltic magma containing ~9 wt.% MgO that ponded at ~21 km (~7 kbar) and fractionated olivine, clinopyroxene, plagioclase and orthopyroxene. Trace element modelling

[2] $Ti_N^* = (Sm_N + Gd_N) / 2$

indicates that during fractionation, these du Chef parent magmas were not contaminated by felsic country rock. Instead, the parent liquids evolved via simple fractional crystallisation, over the course of which, the magma chambers were periodically tapped and liquids removed to form individual du Chef dykes which record the geochemical evolution of the parent magmas. It is however likely that some of these evolved melts became contaminated by the various crustal components into which the du Chef dyke swarm intruded, thus producing some of the HFSE variation observed in **Fig. 9**.

5.3 Primary Magmas and Mantle Source

The relatively evolved nature of the du Chef dykes (MgO ≤ 9 wt.%) suggests that even the most primitive dyke does not represent an unfractionated primary magma derived through partial melting of mantle peridotite. To characterise the primary magmas of such evolved suites, Herzberg and Asimow (2008) developed the PRIMELT2 software which can calculate primary magma compositions for evolved lavas. PRIMELT2 uses forward and inverse models to compute a melt fraction which is capable of, (a) being formed by partial melting of fertile mantle peridotite and (b) producing the major element composition of the evolved lava sample through fractionation or accumulation of olivine alone.

Fractional crystallisation models which use sample DC011 as a parent magma composition predict that olivine is the first mineral to crystallise **(Fig. 8)**. This, along with the ~9 wt.% MgO content of DC011, suggests that this sample could feasibly have evolved solely through olivine fractionation of a primary mantle melt (Herzberg and Asimow 2008). Indeed, the application of PRIMELT2 to sample DC011 produces a successful result, whereby the major element composition of sample DC011 can be replicated by 30% partial melting of fertile mantle peridotite to produce a picritic primary magma containing 19.8 wt.% MgO, 1.92 wt.% $Na_2O + K_2O$, 11.4 wt.% Al_2O_3 and 46.2 wt.% SiO_2 . Fractional crystallisation of this primary magma, such that 32% of it crystallises as olivine, produces a remaining liquid fraction with a major element composition similar to sample DC011. By using these degrees of partial melting and olivine fractionation, we can investigate the possible mantle sources for the du Chef dykes.

Five mantle reservoirs are modelled **(Table 3)**: Depleted MORB Mantle (DMM), Enriched Mantle (EM1 and EM2) and Primitive Mantle (PM) and High $^{238}U/^{204}Pb$ Mantle (HIMU). The composition of DMM has been constrained by Workman and Hart (2005) from the trace

element depletion trends of abyssal peridotites. The compositions of the EM1 and EM2 reservoirs are estimated from inverse modelling of the compositions of EM1 and EM2 basalts from the Tristan da Cuhna, Gough, Samoan and Society islands (Willbold and Stracke 2006). The HIMU reservoir is similarly estimated from inverse modelling using the compositions of basalts from Tubuai, Mangaia and Rurutu (Chauvel et al. 1992). The composition of PM is derived from studies of chondritic meteorites and refractory element ratios of mantle peridotites (McDonough and Sun 1995). It should be noted that projecting the existence of these reservoirs, predominantly recognised from modern intraplate basaltic rocks, back into the Paleoproterozoic is questionable. However, these reservoir compositions can be used to characterise the enriched or depleted nature of the du Chef mantle source region.

The 30% partial melting needed to form the du Chef primary magma (as predicted by the PRIMELT2 model for sample DC011) may be modelled using batch melting **(Equation 4)** for garnet lherzolites (Johnson et al. 1990) from the five different mantle reservoirs described above. Garnet lherzolite was chosen for the models as all of the du Chef dykes have relatively depleted HREE patterns **(Fig. 5)** which indicates that mantle melting occurred within the garnet stability field but was of an insufficient degree to melt all of the garnet in the source. A garnet-bearing source may also be implied by the negative Zr-Hf anomalies observed in the du Chef dykes, which for other intracontinental basaltic rocks, have been interpreted to have been imparted on primary magmas by the segregation of magmas from a mantle plume with residual majorite garnet, at depths of 400 to 600 km (Xie et al. 1993).

The PRIMELT2 model predicts that, following partial melting, 32% of the primary magma crystallised as olivine, with the remaining liquid fraction approximating to the composition of sample DC011. The affects of this fractionation on the trace element chemistry of the primary magmas derived from the three different mantle reservoirs can be calculated using equation 1 and the olivine/melt partition coefficients of Bedard (2001) with 32% fractionation (F = 0.32).

Fig. 11. shows the Primitive Mantle-normalised multi-element patterns for sample DC011 for which PRIMELT2.XLS was able to define partial melting and fractionation parameters. Also plotted are the compositions of magmas formed by fractional crystallisation of primary magmas derived from melting of garnet lherzolites from the DMM, EM1, EM2, HIMU and PM mantle reservoirs using the parameters of melting and fractionation stated above. **Fig. 11.**

shows that a fractionated magma, derived from a primitive mantle garnet lherzolite is an unlikely parent magma for the du Chef dykes as such a liquid is characterised by $(Th/La)_N$ = 1.01- in contrast to sample DC which has a much lower ratio [$(Th/La)_N$ = 0.43]. The modelled fractionated magma derived from the DMM reservoir has a more similar $(Th/La)_N$ ratio to the du Chef dykes but also records distinctly lower trace element abundances (2.2 × primitive mantle) than sample DC011 (5.4 × primitive mantle). The fractionated magma derived from the enriched mantle (EM1 and EM2) reservoirs have very similar element abundances and primitive mantle-normalised patterns as sample DC011 for the least incompatible trace elements as well as comparable $(Th/La)_N$ ratios, but fails to replicate the LREE enrichment observed in the du Chef dykes [$(La/Sm)_N = 1.90 \pm 0.33$] and instead shows slight LREE depletion [$(La/Sm)_N$ = 0.81]. The fractionated magma derived from partial melting of the HIMU reservoir records similar MREE-HREE ratios to sample DC011, but predicts much higher abundances as well as contrasting $(Th/La)_N$ ratios. Further modelling which involves fractionation of primary magmas formed via melting an EM1 garnet lherzolite previously modified by the addition of a crustal component, [as might occur during melting of lower crustal material by hot upwelling mantle (e.g., Xu et al. 2002)], is also unsuccessful in replicating the trace element composition of sample DC011, since the composition of the modelled magma in this instance is characterised by $(Th/La)_N$ ratios > 1 and negative Nb-Ta anomalies.

This indicates that fractional crystallisation of partial melts of the mantle reservoirs described here is not a viable mechanism for producing the parent magma of the du Chef dykes. An alternative source is suggested by the work of Polat et al. (1998) who observed similar trace element characteristics in ultramafic rocks of the late-Archean Schreiber-Hemlo and White River-Dayohessarah greenstone belts of the Superior Craton. In this earlier work, Polat et al. (1998) suggested that primary magmas characterised by trace element signatures like those observed in the du Chef dykes were the product of deep-seated, mantle plume magmas derived from subducted and recycled oceanic lithosphere albeit with a different trace element signature than the HIMU reservoir modelled above.

5.4. Thermal Plume

Using overlapping U-Pb ages of mafic suites, Söderlund et al. (2010) have suggested that the du Chef dyke swarm is correlative with some of the Sebanga dykes preserved on the Zimbabwe craton. Söderlund et al. (2010) used this coeval geochronological data to suggest

that during the late-Archean and early-Proterozoic, the Superior, Karelia and Zimbabwe cratons were 'nearest neighbours' in a larger supercontinent (Ernst and Bleeker 2010; Söderlund et al. 2010) which began to rift apart approximately 2.4 Ga during an episode of mantle plume-driven continental breakup.

Mantle plumes active in the modern era such as those beneath Iceland and Hawaii are characterised by anomalously hot upper mantle hundreds of degrees hotter than the ambient mantle (e.g., Wolfe et al. 1997; Bijwaard and Spakman 1999; Li et al. 2000). For ancient magmatic systems the existence of anomalously high-temperature magmatism (indicative of a mantle plume) can be investigated by examining the geochemistry of primary magmas and calculating their mantle potential temperature (T_P) – the temperature the mantle would reach if it was brought to the surface adiabatically without melting (McKenzie and Bickle 1988). The T_P of the mantle source of a primary magma may be recorded in its petrology and major element geochemical composition and can be inferred by calibration and parameterisation of laboratory data to the magma in question. PRIMELT2.XLS software developed by Herzberg and Asimow (2008) can be used to calculate T_p. Once PRIMELT2.XLS obtains a primary magma composition, the MgO concentration is used to calculate T_P where the total uncertainty due to potential errors in determining the MgO content of primary magmas is ± 60°C (2σ) (Herzberg and Asimow 2008; Herzberg et al. 2010).

PRIMELT2.XLS was able to calculate the potential temperature of 1567°C for sample DC011. By comparing this potential temperature with temperature estimates of the ambient upper mantle in the Paleoproterozoic, we can determine whether the magmatism which formed the du Chef dykes was derived from an anomalously hot upper mantle (i.e., plume) as is predicted by mantle plume theory (Campbell 2007), and confirmed by observations of the mantle beneath Hawaii and Iceland (Bijwaard and Spakman 1999; Li et al. 2000) and elsewhere (Montelli et al. 2004; Waite et al. 2006).

There is a general consensus that the mantle was significantly hotter during the Paleoproterozoic than it is today **(Fig. 12)**. Exactly how much hotter is a contentious point as different models predict different cooling histories for the Earth. Richter (1988) presents models in which the starting temperature of the upper mantle at 4.5 Ga was either 2000°C or 2500°C which cooled at a continuously decreasing rate to reach a present day value of 1350°C. Regardless of the two starting temperatures used by Richter (1988), his model

predicts that at ~2.4 Ga the temperature of the ambient upper mantle was ~1480°C. Korenaga (2008) has proposed a model which is characterised by an initial increase in mantle T_P from ~1650°C at 4.5 Ga to ~1700°C at 3.6 Ga. This initial temperature increase is followed by an increasingly rapid drop in T_P to a present day values of 1350°C. Davies (2009) suggests that the low Urey ratio (heat produced by radioactive decay/heat loss) used by Korenaga (2008) is extreme and instead favours a model of constantly decreasing temperature from an initial upper mantle temperature of 1800°C at 4.5 Ga to reach a modern day temperature of 1300°C.

These three secular cooling curves are plotted on **Fig. 12** along with the T_P of sample DC011 (1567°C). This sample records a T_p 87°C and 179°C higher than is predicted for the ~2.4 Ga mantle by the models of Richter (1988) and Davies (2009) respectively, but 138°C lower than is predicted by the model of Korenaga (2008). Determining the veracity of the disparate models presented in **Fig. 12** is beyond the scope of this study. However, the model of Korenaga (2008) has been seriously challenged by Davies (2009) and Karato (2010). Davies (2009) disagrees with the assumption of Korenaga (2008) that plate thickness is determined by dehydration during melting at mid-ocean ridges and instead suggests that plate thickness is determined by conductive cooling. Davies (2009) also argues that the model of Korenaga (2008) is overly sensitive to the radius of curvature of bending plates at subduction zones. Karato (2010) demonstrates that plate curvature at subduction zones depends on the flexural rigidity which in turn, depends on plate thickness. This finding by Karato (2010) essentially invalidates the model of Korenaga (2008) who assumes that the radius of curvature of bending plates remains constant. On this basis therefore we prefer the models of Richter (1988) and Davies (2009) in estimating the temperature of the upper mantle during the emplacement of the du Chef dykes at ~2.4 Ga.

Other studies have estimated the temperature of the upper mantle at various points during the Archean (e.g., Ohta et al. 1996; Galer and Mezger 1998; Komiya et al. 2004). Galer and Mezger (1998) examined the regional metamorphic grade of ten undisturbed Archean granite-greenstone segments and showed that metamorphic facies exposed at the surface today are indicative of burial pressures of ~1.5 kbar. From these burial pressures, Galer and Mezger (1998) infer that, since 3 Ga, the undisturbed portions of cratons have been uplifted ~5 km, implying a mean continental thickness of ~46 km when the cratons were stabilised at ca. 2.5 Ga (Bleeker 2003). Galer and Mezger (1998) argue that during the Archean, in order to maintain isostatic equilibrium with the cratons, the oceanic crust would have had to have

been ~14 km thick (assuming a relatively fixed cratonic mass through time). Under these conditions, Galer and Mezger (1998) infer an upper mantle temperature of ~90 °C hotter than the present day at 3 Ga. Using a linear cooling rate of 30 °C Gy^{-1} (which is comparable to estimates of the present day cooling rate of the Earth), the temperature of the upper mantle at 2.4 Ga can be estimated as 1422 °C.

Ohta et al. (1996) used the geochemistry of Archean MORB-like rocks preserved in a 3.1-3.3 Ga accretionary complex in Pilbara, Western Australia to constrain the ambient temperature of the upper mantle at 3.1-3.3 Ga to be 1400 °C. Using this temperature of 1400 °C as an estimate for T_P at 3.2 Ga and a simplistic, linear cooling modelling between 1400 °C at 3.2 Ga and 1350 °C today, the temperature of the mantle at 2.4 Ga can be estimated at 1387 °C. In a similar study, Komiya et al. (2004) use the geochemistry of Archean MORB rocks preserved in the 3.8 Ga Isua Supracrustal Belt, southwest Greenland to constrain upper mantle temperatures at that time to be ~1480 °C. Again, using a simplistic, linear cooling model between 1480 °C at 3.8 Ga and 1350 °C today, the temperature of the upper mantle at 2.46 Ga can be estimated at 1432 °C. These three estimates of upper mantle temperature at ~2.4 Ga using the work of Ohta et al. (1996), Galer and Mezger (1998) and Komiya et al. (2004) are all significantly lower than the T_P recorded by sample DC011 (180 °C, 135 °C and 145 °C respectively). This reinforces the evidence summarised in **Fig. 12** that the du Chef dyke swarm formed from anomalously hot source, consistent with a mantle plume.

In summary, secular cooling models of the Earth's mantle suggest that the du Chef dykes originated from anomalously hot early-Proterozoic mantle according to the models of Davies (2009) and Richter (1988) as well as other estimates derived from studies of Archean mantle rocks (Ohta et al. 1996; Galer and Mezger 1998; Komiya et al. 2004). This evidence, along with consistent trace element geochemistry suggests that the du Chef dykes are the product of mantle plume-driven magmatism as proposed by Ernst and Buchan (2004) and Söderlund et al. (2010). However, alternate models of the cooling of the mantle [e.g., Korenaga (2008) and Abbot et al. (1994)] suggest that the du Chef dykes are not the product of an anomalously hot mantle plume. Continued research into the thermal evolution of the mantle and derivation of robust models which estimate the temperature of the upper mantle at ~2.4 Ga will help better determine the nature of the source and petrogenesis of the du Chef dykes.

5.5. Correlative units

Based on coeval U-Pb ages, other workers have proposed that the du Chef dykes may be genetically linked to the 2408 ± 2 Ma Sebanga dykes preserved on the Zimbabwe craton (Söderlund et al. 2010), as well as potentially to the 2403 ± 3 Ma Ringvassøy dykes on the Kola-Karelia craton (Kullerud et al. 2006), the 2410 ± 2 Ma Widgiemooltha swarm of the Yilgarn craton (Doehler and Heaman 1998), and the 2418 ± 3 Ma Scourie dyke swarm in northwest Scotland (Nemchin and Pidgeon 1998). These other igneous provinces are comprised of numerous predominantly doleritic intrusions and are similar to the du Chef dyke swarm in terms of areal extent and their continental tholeiitic basalt geochemical affinities (Kullerud et al. 2006; Hughes et al. submitted). Together with the du Chef dyke swarm, these suites may represent a hitherto unknown early Proterozoic Large Igneous Province (Ernst and Buchan 2002).

Comparisons of the currently available trace element geochemistry of the du Chef dykes and their potential correlative suites **(Fig. 13)** reveal some interesting features. Firstly, there is a striking similarity between all of the suites in terms of their general enrichments in the most incompatible REE relative to the least incompatible elements. Of the three suites potentially correlative with the du Chef swarm, it is the Scourie dykes which have the most similar trace element geochemistry to the du Chef dykes. These two dyke swarms share comparable average trace element abundances as well as similarly large Zr-Hf and Y anomalies, which may indicate the two swarms were derived from a common mantle reservoir that underwent a similar degree of partial melting. However, in contrast to the du Chef dykes, both the Ringvassøy and Scourie dykes all have high $(Th/La)_N$ ratios and are characterised by significant, negative Nb-Ta anomalies.

The trace element signatures of these three suites are common in igneous rocks formed in modern volcanic arc settings (e.g., Pearce and Peate 1995). Thus, when observed in Paleoproterozoic igneous rocks, these signatures have often been interpreted as evidence of formation in such an environment (e.g., Van Boening and Nabelek 2008). However, the volcanic arc-like trace element compositions recorded by the du Chef dykes are common in the palaoeproterozoic igneous record and are observed in rocks of a similar age which preserve field evidence that entirely precludes a subduction-related setting including radiating dyke swarms and flood basalt provinces (Phinney and Halls 2001; Jolly 1987). For such suites which record trace element signatures like those observed in the dykes potentially correlative with du Chef, alternative petrogenetic mechanisms which may impart an arc-like

trace element geochemistry have been suggested. Potential explanations include; (1) partial melting of subduction-modified sub-continental lithospheric mantle (Sandeman and Ryan 2008); (2) a widespread ancient mantle reservoir, fundamentally different to those observed in the modern mantle (Vogel et al. 1998); or, (3) the contamination of mantle melts by continental crust during fractionation in deep crustal magma chambers (e.g., Nelson et al. 1990).

Thus the differences in the trace element chemistry observed between the du Chef swarm and its potential correlative suites do not necessarily rule out a cogenetic origin. Instead, these differences may be the product of melting of a compositionally heterogeneous mantle plume head that had sampled various mantle reservoirs or lithospheric components during its transit through the crust and mantle, (cf., Kerr et al. 2002; Ketchum et al. 2013) or potentially through contrasting evolutionary histories of cogenetic mantle melts in disparate crustal magma chambers (Bleeker 2004). Further work aimed at better defining the ages of these coeval suites would better constrain any potential temporal link, while further palaeomagnetic work would characterise the possibility of a 'nearest neighbour' situation (Bleeker 2003) between the suites at ~2.4 Ga **(Fig. 14)**.

6. Summary and conclusions

1. The primary magmas of the du Chef were low-Ti, low-Al picritic basalts, derived from partial melting of a garnet-bearing mantle peridotite similar in trace element composition (but more enriched) to the modern-day HIMU reservoir.
2. The magmas produced by this partial melting were significantly higher in temperature than the ambient mantle and may indicate the presence of a mantle plume beneath the Superior craton during the early Proterozoic.
3. Prior to intrusion of the dykes, the du Chef primary magmas ponded in mid-deep level crustal chambers where they fractionated olivine, clinopyroxene, plagioclase and orthopyroxene but with little assimilation of host rocks. These mid-deep level crustal chambers were periodically tapped, with fractions of melt migrating from the chambers to be emplaced as individual du Chef dykes.
4. Magmas in individual dykes were contaminated insitu by the host rocks and inherited variable, but minor, negative anomalies in some of the HFSE.

5. Units proposed to be correlative with the du Chef dykes have slightly different geochemical compositions that may be the result of differences in source reservoir or contamination by crust or lithospheric mantle

7. Acknowledgements

This study forms part of a Ph.D. dissertation undertaken by T.J.R.C. at the University of Cardiff, United Kingdom. A. Okrugin's assistance in the field is acknowledged. J. Strongman, J. Fletcher and J. Pett are thanked for their permission of use of the petrographic equipment at Petrolab Ltd. L. Badham, A. Oldroyd, L. Woolley and P. Fisher are thanked for their help in preparation and analysis of samples.

8. References

Abbott, D., Burgess, L., Longhi, J. and Smith W. H. F., 1994. An empirical thermal history of the Earth's upper mantle. *Journal of Geophysical Research*, 99, 13835–13850

Asimow, P. D., and Ghiorso, M. S., 1998. Algorithmic modifications extending MELTS to calculate subsolidus phase relations. *American Mineralogist,* 83, 1127–1132.

Bédard, J., 2001. Parental magmas of the Nain Plutonic Suite anorthosites and mafic cumulates: a trace element modelling approach. *Contributions to Mineralogy and Petrology,* 141**,** 747-771.

Bijwaard, H. and Spakman, W., 1999. Tomographic evidence for a narrow whole mantle plume below Iceland. *Earth and Planetary Science Letters,* 166**,** 121-126.

Bleeker, W., 2003. The late Archean record: a puzzle in ca. 35 pieces. *Lithos,* 71**,** 99-134.

Bleeker, W., 2004. Taking the pulse of planet Earth: a proposal for a new multi-disciplinary flagship project in Canadian solid Earth sciences. *Geoscience Canada,* 31**,** 179-190.

Boudreau, A. E., 1999. PELE-a version of the MELTS software program for the PC platform. *Comput. Geosci.,* 25**,** 201-203.

Campbell, I. H., 2007. Testing the plume theory. *Chemical Geology,* 241**,** 153-176.

Cann, J. R., 1970. Rb, Sr, Y, Zr and Nb in some ocean floor basaltic rocks. *Earth and Planetary Science Letters,* 10**,** 7-11.

Card, K. D., 1990. A review of the Superior Province of the Canadian Shield, a product of Archean accretion. *Precambrian Research,* 48**,** 99-156.

Chauvel, C., Hofmann, A. W. and Vidal, P., 1992. HIMU-EM: The French Polynesian connection. *Earth and Planetary Science Letters,* 110**,** 99-119.

Ciesielski A., and Madore. C., 1989. Litho-tectonic map of the Grenville Front, the Archean parautochthonous orthogneisses and Proterozoic dykes in the Central Grenville Province southeast of Chibougamau, Québec. In *Open File* 2059. Geological Survey of Canada.

Ciesielski, A. 1991. Litho-tectonic map of the Grenville Front, southeast of Val d'Or, Québec. In *Open File* 2397. Geological Survey of Canada.

Condie, K.C., 2005. High field strength element ratios in Archean basalts - a window to evolving sources of mantle plumes? *Lithos*, 79, 491-504.

Davies, G. F., 2009. Effect of plate bending on the Urey ratio and the thermal evolution of the mantle. *Earth and Planetary Science Letters,* 287**,** 513-518.

DePaolo, D.J., 1981. Trace element and isotopic effects of combined wallrock assimilation and fractional crystallization: *Earth and Planetary Science Letters*, 53, 189-202.

Doehler, J.S., and Heaman L.M., 1998. 2.41 Ga U–Pb baddeleyite ages for two gabbroic dykes from the Widgiemooltha Swarm, Western Australia. A Yilgarn–Lewisian connection? *Geological Society of America 1998 Annual Meeting, Abstracts with Programs, Geological Society of America,* 30, 291–292.

Dufrechou, G.; Harris, L.B., 2013.Tectonic models for the origin of regional transverse structures in the Grenville Province of SW Québec interpreted from regional gravity. *Journal of Geodynamics* 64, 15-39.

Ernst, R. E. and Buchan, K. L., 2002. Maximum size and distribution in time and space of mantle plumes: evidence from large igneous provinces. *Journal of Geodynamics,* 34 309-342.

Ernst, R. E. and Buchan, K. L., 2004. Large Igneous Provinces (LIPs) in Canada and adjacent regions: 3 Ga to Present. *Geoscience Canada,* 31**,** 103-126.

Ernst, R. E. and Bleeker, W., 2010. Large igneous provinces (LIPs), giant dyke swarms, and mantle plumes: significance for breakup events within Canada and adjacent regions from 2.5 Ga to the Present. *Canadian Journal of Earth Sciences,* 47**,** 695-739.

Galer, S. J. G. and Mezger, K., 1998. Metamorphism, denudation and sea level in the Archean and cooling of the Earth. *Precambrian Research,* 92**,** 389-412.

Ghiorso, M. S. and Sack, R. O., 1995. Chemical mass transfer in magmatic processes IV. A revised and internally consistent thermodynamic model for the interpolation and extrapolation of liquid-solid equilibria in magmatic systems at elevated temperatures and pressures. *Contributions to Mineralogy and Petrology,* 119**,** 197-212.

Herzberg, C. and Asimow, P. D., 2008. Petrology of some oceanic island basalts: PRIMELT2.XLS software for primary magma calculation. *Geochem. Geophys. Geosyst.,* 9**,** Q09001.

Herzberg, C., Condie, K. and Korenaga, J., 2010. Thermal history of the Earth and its petrological expression. *Earth and Planetary Science Letters,* 292**,** 79-88.

Hughes, H. S. R., McDonald, I., Goodenough, K. M., Kerr, A. C. and Ciborowski, T. J. R., (submitted). Geochemistry of the Scourie Dyke Suite: Evidence for parental magma sources and insights into the Lewisian lithospheric mantle, NW Scotland, *Lithos*

Johnson, K. T. M., Dick, H. J. B. and Shimizu, N., 1990. Melting in the oceanic upper mantle: an ion microprobe study of diopsides in abyssal peridotites. *Journal of Geophysical Research,* 95**,** 2661-2678.

Jolly, W. T., 1987. Geology and geochemistry of Huronian rhyolites and low-Ti continental tholeiites from the Thessalon region, central Ontario. *Canadian Journal of Earth Sciences,* 24**,** 1360-1385.

Karato, S.-i., 2010. Rheology of the deep upper mantle and its implications for the preservation of the continental roots: A review. *Tectonophysics,* 481**,** 82-98.

Kerr, A. C., Tarney, J., Kempton, P. D., Spadea, P., Nivia, A., Marriner, G. F. and Duncan, R. A., 2002. Pervasive mantle plume head heterogeneity: Evidence from the late Cretaceous Caribbean-Colombian oceanic plateau. *Journal of Geophysical Research: Solid Earth,* 107**,** ECV 2-1-ECV 2-13.

Ketchum K. Y., Heaman L. M., Bennett G., and Hughes, D., 2013. Age, petrogenesis and tectonic setting of the Thessalon volcanic rocks, Huronian Supergroup, Canada. *Precambrian Research,* 233, 144-172.

Komiya, T., Maruyama, S., Hirata, T., Yurimoto, H. and Nohda, S., 2004. Geochemistry of the oldest MORB and OIB in the Isua Supracrustal Belt, southern West Greenland: Implications for the composition and temperature of early Archean upper mantle. *Island Arc,* 13**,** 47-72.

Korenaga, J., 2008. Urey ratio and the structure and evolution of Earth's mantle. Reviews of Geophysics, 46, 1-32.

Kullerud, K., Skjerlie, K. P., Corfu, F. and de la Rosa, J.D., 2006. The 2.40 Ga Ringvassøy mafic dykes, West Troms Basement Complex, Norway: The concluding act of early Paleoproterozoic continental breakup. *Precambrian Research*, 150, 183-200.

Krogh, T. E., 1994. Precise U-Pb ages for Grenvillian and pre-Grenvillian thrusting of Proterozoic and Archean metamorphic assemblages in the Grenville Front tectonic zone, Canada. *Tectonics,* 13**,** 963-982.

Kulikov, V. S., Bychkova, Y. V., Kulikova, V. V. and Ernst, R., 2010. The Vetreny Poyas (Windy Belt) subprovince of southeastern Fennoscandia: An essential component of the ca. 2.5–2.4 Ga Sumian large igneous provinces. *Precambrian Research,* 183**,** 589-601.

Leclerc, F., Bédard, J. H., Harris, L. B., McNicoll, V. J, Goulet, N., Roy, P., and Houle., 2011. Tholeiitic to calc-alkaline cyclic volcanism in the Roy Group, Chibougamau area, Abitibi Greenstone Belt — revised stratigraphy and implications for VHMS exploration. *Canadian Journal of Earth Sciences*, 48, 661-694.

Li, X., Kind, R., Priestley, K., Sobolev, S. V., Tilmann, F., Yuan, X. and Weber, M., 2000. Mapping the Hawaiian plume conduit with converted seismic waves. *Nature,* 405**,** 938-941.

Martignole, J. and Martelat, J.-E., 2005. Proterozoic mafic dykes as monitors of HP granulite facies metamorphism in the Grenville Front Tectonic Zone (western Québec). *Precambrian Research,* 138**,** 183-207.

McDonough, W. F. and Sun, S. S., 1995. The composition of the Earth. *Chemical Geology,* 120**,** 223-253.

McKenzie, D. and Bickle, M. J., 1988. The volume and composition of melt generated by extension of the lithosphere. *Journal of Petrology,* 29**,** 625-679.

Minifie, M. J., Kerr, A. C., Ernst, R. E., Hastie, A. R., Ciborowski, T. J. C., Desharnais, G. and Milliar, I. L., 2013. The northern and southern sections of the western ca. 1880 Ma Circum-Superior Large Igneous Province, North America: The Pickle Crow dyke connection? *Lithos*, 174, 217-235.

Montelli, R., Nolet, G., Dahlen, F. A., Masters, G., Engdahl, E. R., and Hung, S-H., 2004. Finite-Frequency Tomography Reveals a Variety of Plumes in the Mantle. Science, 16, 338-343.

Nelson, D. O., Morrison, D. A. and Phinney, W. C., 1990. Open-system evolution versus source control in basaltic magmas: Matachewan-Hearst dike swarm, Superior Province, Canada. *Canadian Journal of Earth Sciences,* 27, 767-783.

Nemchin, A. A. and Pidgeon, R. T., 1998. Precise conventional and SHRIMP baddeleyite U‐Pb age for the Binneringie Dyke, near Narrogin, Western Australia, *Australian Journal of Earth Sciences*, 45, 673-675.

Ohta, H., Maruyama, S., Takahashi, E., Watanabe, Y. and Kato, Y., 1996. Field occurrence, geochemistry and petrogenesis of the Archean Mid-Oceanic Ridge Basalts (AMORBs) of the Cleaverville area, Pilbara Craton, Western Australia. *Lithos,* 37**,** 199-221.

Pearce, J. A., 1996. A user's guide to basalt discrimination diagrams. In *Trace element geochemistry of volcanic rocks: appliction for massive sulphide exploration,* ed. D. Wyman, 79-113. Winnipeg: Geological Association of Canada, Mineral Deposits Division.

Pearce, J. A. and Peate, D. W., 1995. Tectonic implications of the composition of volcanic arc magmas *Annual review of Earth and planetary sciences,* 23**,** 251-285.

Phinney, W. C. and Halls, H. C., 2001. Petrogenesis of the Early Proterozoic Matachewan dyke swarm, Canada, and implications for magma emplacement and subsequent deformation. *Canadian Journal of Earth Sciences,* 38**,** 1541-1563.

Polat, A., Kerrich, R., and Wyman, D. A., 1998. The late Archean Schreiber-Hemlo and White River-Dayohessarah greenstone belts, Superior Province: Collages of oceanic plateaus, oceanic island arcs, and subduction-accretion complexes. *Tectonophysics* 289, 295-326.

Pirajno, F. and Hoatson, D.M., 2012. A review of Australia's Large Igneous Provinces and associated mineral systems: Implications for mantle dynamics through geological time. *Ore Geology Reviews* 48, 2-54.

Richter, F. M., 1988. A Major Change in the Thermal State of the Earth at the Archean-Proterozoic Boundary: Consequences for the Nature and Preservation of Continental Lithosphere. *Journal of Petrology,* Special_Volume**,** 39-52.

Rudnick, R. L. and Gao, S., 2003. 3.01 - Composition of the Continental Crust. In *Treatise on Geochemistry,* eds. D. H. Editors-in-Chief: Heinrich and K. T. Karl, 1-64. Oxford: Pergamon.

Sandeman, H. A. and Ryan, J. J., 2008. The Spi Lake Formation of the central Hearne domain, western Churchill Province, Canada: an axial intracratonic continental tholeiite trough above the cogenetic Kaminak dyke swarm. *Canadian Journal of Earth Sciences,* 45**,** 745-767.

Söderlund, U., Hofmann, A., Klausen, M. B., Olsson, J. R., Ernst, R. E. and Persson, P.-O., 2010. Towards a complete magmatic barcode for the Zimbabwe craton: Baddeleyite U–Pb dating of regional dolerite dyke swarms and sill complexes. *Precambrian Research,* 183**,** 388-398.

Stachel, T., Banas, A., Muehlenbachs, K., Kurszlaukis, S. and Walker, E.C., 2006. Archean diamonds from Wawa (Canada): samples from deep cratonic roots predating cratonization of the Superior Province. *Contributions to Mineralogy and Petrology*, 151, 737-750.

Sun, S. –s., McDonough, W. F., 1989. Chemical and isotopic systematics of oceanic basalts: implications for mantle composition and processes, *Geological Society, London, Special Publications*, 42, 313-345.

Thériault, R., Beauséjour, S. and Tremblay, A., 2012. MAP: Geology of Québec DV2012-7. Ministère des Ressources naturelles. Direction générale de Géologie Québec

Van Boening, A. M. and Nabelek, P. I., 2008. Petrogenesis and tectonic implications of Paleoproterozoic mafic rocks in the Black Hills, South Dakota. *Precambrian Research,* 167**,** 363-376.

Vogel, D. C., Vuollo, J. I., Alapieti, T. T. and James, R. S., 1998. Tectonic, stratigraphic, and geochemical comparisons between ca. 2500-2440 Ma mafic igneous events in the Canadian and Fennoscandian Shields. *Precambrian Research,* 92**,** 89-116.

Waite, G. P., Smith, R. B. and Allen, R. M., 2006. V_P and V_S structure of the Yellowstone hot spot from teleseismic tomography: Evidence for an upper mantle plume. *Journal of Geophysical Research*, 111, B04303.

Willbold, M. and Stracke, A., 2006. Trace element composition of mantle end-members: Implications for recycling of oceanic and upper and lower continental crust. *Geochem. Geophys. Geosyst.,* 7**,** Q04004.

Wolfe, C. J., Bjarnason, I. T., VanDecar, J. C. and Solomon, S. C., 1997. Seismic structure of the Iceland mantle plume. *Nature,* 385, 245-247.

Workman, R. K. and Hart, S. R., 2005. Major and trace element composition of the depleted MORB mantle (DMM). *Earth and Planetary Science Letters,* 231, 53-72.

Xie, Q., Kerrich, R. and Fan, J., 1993. HFSE/REE fractionations recorded in three komatiite-basalt sequences, Archean Abitibi greenstone belt: Implications for multiple plume sources and depths. *Geochimica et Cosmochimica Acta,* 57, 4111-4118.

Xu, J-F., Shinjo, R., Defant, M. J., Wang, Q. and Rapp, R. P., 2002. Origin of Mesozoic adakitic intrusive rocks in the Ningzhen area of east China: Partial melting of delaminated lower continental crust? *Geology*, 30, 1111-1114.

- Geochemical characterisation of a previously unstudied Paleoproterozoic, intracontinental, tholeiitic dyke swarm.
- Identification of a Paleoproterozoic thermal plume beneath the Superior Province.
- We have proved the existence of enriched, OIB-like mantle reservoirs during the Paleoproterozoic.
- We present a new palaeoproterozoic continental reconstruction.

Sample	DC001	DC002	DC003	DC004	DC005	DC006	DC007	DC008	DC010	DC011	DC013	DC014	DC015	DC016	DC017	DC018	DC019	DC020
UTM (E)	550620	550653	560353	565583	573015	573462	548834	552965	552965	585722	584705	584680	581748	578738	578768	582583	582578	582595
UTM (N)	5497068	5497125	5479443	5471571	5467189	5466863	5463730	5458295	5458295	5459991	5460291	5460299	5468324	5481228	5481245	5482545	5482500	5483019
Majors (wt.%)																		
SiO_2	45.57	47.40	45.04	47.88	52.01	47.13	47.82	47.43	45.90	47.60	48.13	46.15	45.70	45.32	45.69	48.03	47.82	48.06
TiO_2	2.38	1.62	2.47	1.54	1.02	1.66	1.61	1.33	1.30	1.17	1.17	1.58	2.60	2.69	2.20	1.11	1.20	1.46
Al_2O_3	14.40	14.35	13.50	14.70	14.41	15.65	13.28	15.69	15.52	15.33	13.79	14.56	13.97	12.34	14.12	15.25	15.47	15.69
Fe_2O_3	15.94	14.88	18.56	14.38	12.20	14.16	16.21	12.03	12.32	11.92	14.66	16.56	17.70	19.68	17.61	14.00	14.74	13.01
MnO	0.22	0.20	0.23	0.19	0.17	0.17	0.22	0.15	0.18	0.15	0.19	0.20	0.22	0.23	0.21	0.18	0.19	0.16
MgO	5.73	6.04	5.37	6.39	5.95	7.23	6.29	7.87	8.04	9.02	6.40	6.76	5.76	7.13	5.87	8.88	7.42	6.82
CaO	9.92	9.63	8.55	9.45	9.81	9.85	8.99	10.34	10.50	11.66	10.38	9.40	9.27	9.99	9.24	10.05	10.10	9.65
Na_2O	2.38	2.14	2.75	2.55	2.46	3.25	2.78	2.53	2.42	2.26	2.45	2.37	2.19	2.18	2.23	2.17	2.20	2.64
K_2O	1.21	1.10	1.20	0.85	0.91	0.58	0.95	0.70	1.26	0.35	0.64	0.67	0.92	0.56	0.63	0.36	0.34	0.55
P_2O_5	0.31	0.30	0.27	0.19	0.07	0.22	0.38	0.15	0.15	0.14	0.17	0.21	0.42	0.21	0.28	0.10	0.12	0.18
LOI	1.58	1.48	1.27	0.89	0.82	1.21	0.57	1.66	2.21	1.36	0.71	0.93	1.54	0.42	1.93	0.25	0.47	0.55
Total	99.64	99.12	99.21	99.01	99.84	101.13	99.09	99.88	99.80	100.95	98.69	99.40	100.29	100.74	100.03	100.38	100.05	98.76
Traces (ppm)																		
Sc	37.3	39.2	40.9	39.5	41.0	29.7	35.2	26.1	25.5	27.5	46.0	35.9	35.8	49.2	32.5	35.0	36.9	27.0
Zr	156.1	135.9	131.5	67.7	54.6	89.0	161.7	82.1	88.4	67.3	69.0	64.7	148.9	87.9	115.4	50.7	49.7	92.6
V	325.6	262.1	398.1	225.9	241.4	203.8	161.2	177.0	180.1	177.7	202.7	232.5	256.4	391.5	221.2	203.6	226.0	219.2
Cr	97.9	106.9	42.6	118.3	153.1	89.5	117.4	186.6	179.3	228.1	134.3	76.0	168.9	205.5	70.5	202.6	108.7	95.2
Co	52.4	49.9	56.5	50.4	41.3	57.1	52.2	50.0	46.0	47.0	53.0	61.5	52.6	61.3	54.7	59.8	54.3	49.6
Ni	72.3	81.4	109.7	137.3	121.5	121.9	78.1	171.8	185.5	186.5	52.3	92.6	411.9	133.1	81.3	430.4	116.0	123.3
Cu	92.0	80.9	106.6	88.8	94.5	77.3	78.4	74.0	57.6	55.9	75.7	85.2	88.1	109.5	88.4	82.4	99.4	78.1
Ga	20.5	18.3	21.9	18.0	15.8	18.1	18.9	17.7	16.5	16.2	17.5	18.0	20.2	19.3	20.7	15.6	17.2	18.6
Rb	30.1	25.9	20.0	7.1	19.7	9.5	15.9	5.5	18.5	9.9	8.3	5.7	14.5	7.9	9.7	5.6	4.8	10.0
Sr	260.5	217.9	242.9	298.6	173.0	325.8	258.4	306.1	233.6	293.0	246.7	257.3	236.6	234.4	260.1	225.5	228.7	321.6
Y	31.8	27.2	31.9	26.4	22.2	23.9	40.1	20.0	20.5	17.2	24.1	26.2	43.4	29.1	33.1	18.7	20.1	21.5
Nb	9.47	5.33	9.48	4.55	3.40	7.15	11.54	5.89	5.70	4.73	3.59	3.49	12.93	6.43	8.90	3.34	3.29	6.45
La	17.12	12.29	14.11	8.24	5.81	10.51	19.61	10.31	7.90	7.56	7.82	9.42	20.10	9.16	12.89	5.67	6.30	11.14
Ce	38.44	27.68	30.87	17.48	10.59	23.69	43.00	19.72	18.22	15.80	17.48	18.75	38.29	21.22	29.56	12.22	12.88	22.23
Pr	5.15	3.82	4.31	2.56	1.59	3.32	5.86	2.74	2.52	2.23	2.47	2.71	5.23	3.04	4.12	1.71	1.84	3.02
Nd	22.39	17.01	19.10	11.59	7.41	14.64	25.68	11.99	11.55	10.15	11.55	12.59	23.28	14.17	18.32	7.93	8.70	13.57
Sm	5.23	4.07	4.79	3.06	2.32	3.59	6.25	3.11	3.05	2.67	3.18	3.37	5.83	3.76	4.66	2.22	2.53	3.49
Eu	1.76	1.60	1.76	1.23	0.86	1.32	2.07	1.11	1.06	0.94	1.22	1.31	1.91	1.49	1.72	0.89	2.90	1.24
Gd	5.29	4.20	4.92	3.29	2.57	3.69	6.30	3.16	3.11	2.66	3.28	3.45	6.01	3.98	4.73	2.36	2.64	3.46
Tb	0.86	0.70	0.83	0.59	0.48	0.60	1.05	0.53	0.55	0.46	0.58	0.62	1.05	0.70	0.82	0.43	0.48	0.59
Dy	5.19	4.41	5.14	3.88	3.19	3.68	6.36	3.21	3.43	2.74	3.76	3.94	6.59	4.44	5.16	2.89	3.07	3.60
Ho	0.99	0.85	0.98	0.77	0.63	0.69	1.22	0.60	0.63	0.52	0.74	0.77	1.29	0.86	0.99	0.57	0.61	0.67
Er	2.72	2.39	2.73	2.16	1.78	1.93	3.34	1.64	1.74	1.45	2.12	2.21	3.67	2.46	2.86	1.65	1.78	1.84
Tm	0.43	0.38	0.43	0.35	0.30	0.30	0.54	0.26	0.27	0.22	0.34	0.35	0.59	0.38	0.45	0.27	0.29	0.29
Yb	2.91	2.59	2.94	2.37	2.02	1.98	3.57	1.67	1.74	1.43	2.22	2.33	3.87	2.55	2.96	1.76	1.96	1.91
Lu	0.44	0.41	0.45	0.37	0.30	0.30	0.54	0.25	0.25	0.21	0.33	0.35	0.59	0.38	0.44	0.27	0.30	0.29
Hf	3.72	3.14	3.18	1.85	1.54	2.27	3.77	2.17	2.11	1.74	1.93	1.78	3.94	2.35	3.08	1.47	1.41	2.27
Ta	0.68	0.36	0.62	0.32	0.23	0.48	0.81	0.41	0.40	0.33	0.24	0.23	0.88	0.44	0.60	0.22	0.23	0.46
Pb	4.11	4.57	10.32	4.12	4.07	5.44	4.82	5.58	7.76	2.20	2.22	3.06	4.31	2.60	2.20	0.64	31.91	1.52
Th	1.16	0.72	0.60	0.33	0.38	0.59	0.83	0.58	0.51	0.41	0.30	0.23	1.19	0.43	0.73	0.27	0.22	0.61
U	0.29	0.20	0.22	0.18	0.18	0.15	0.24	0.16	0.16	0.12	0.08	0.07	0.31	0.10	0.18	0.07	0.12	0.17

Table 1. Geochemical data for the du Chef dykes studied

Model	Pressure	H_2O content	Oxygen buffer
Model 1	1 kbar	0%	QFM
Model 2	1 kbar	1%	QFM
Model 3	3 kbar	0%	QFM
Model 4	5 kbar	0%	QFM
Model 5	7 kbar	0%	QFM
Model 6	10 kbar	0%	QFM

Table 2. Model parameters used in Pele for investigation fractional crystallisation of sample DC011

Element (ppm)	DMM	EM1	EM2	HIMU	PM
Th	0.01	0.03	0.04	0.04	0.09
Nb	0.15	0.38	0.37	0.69	0.71
Ta	0.01	0.03	0.03	0.04	0.04
La	0.19	0.60	0.61	0.77	0.69
Ce	0.55	1.75	1.77	2.29	1.78
Pr	0.11	0.29	0.29	0.41	0.28
Nd	0.58	1.47	1.48	2.26	1.35
Zr	5.00	13.00	13.00	22.00	11.00
Hf	0.16	0.36	0.37	0.63	0.31
Sm	0.24	0.52	0.52	0.84	0.44
Eu	0.10	0.20	0.20	0.33	0.17
Ti	716	1433	1457	2437	1300
Gd	0.36	0.72	0.73	1.19	0.60
Tb	0.07	0.13	0.14	0.22	0.11
Dy	0.51	0.92	0.94	1.52	0.74
Y	3.33	5.77	5.88	9.50	4.55
Ho	0.12	0.20	0.21	0.34	0.16
Er	0.35	0.60	0.61	1.00	0.48
Tm	0.05	0.09	0.09	0.15	0.07
Yb	0.37	0.62	0.63	1.04	0.49
Lu	0.06	0.10	0.10	0.16	0.07

Table 3. Trace element compositions of mantle end-members modelled in this study. Data sources: DMM – Workman and Hart (2005), EM1 – Willbold and Stracke (2006), EM2 – Willbold and Stracke (2006), HIMU – Chauvel et al. (1992), PM – McDonough and Sun (1995).

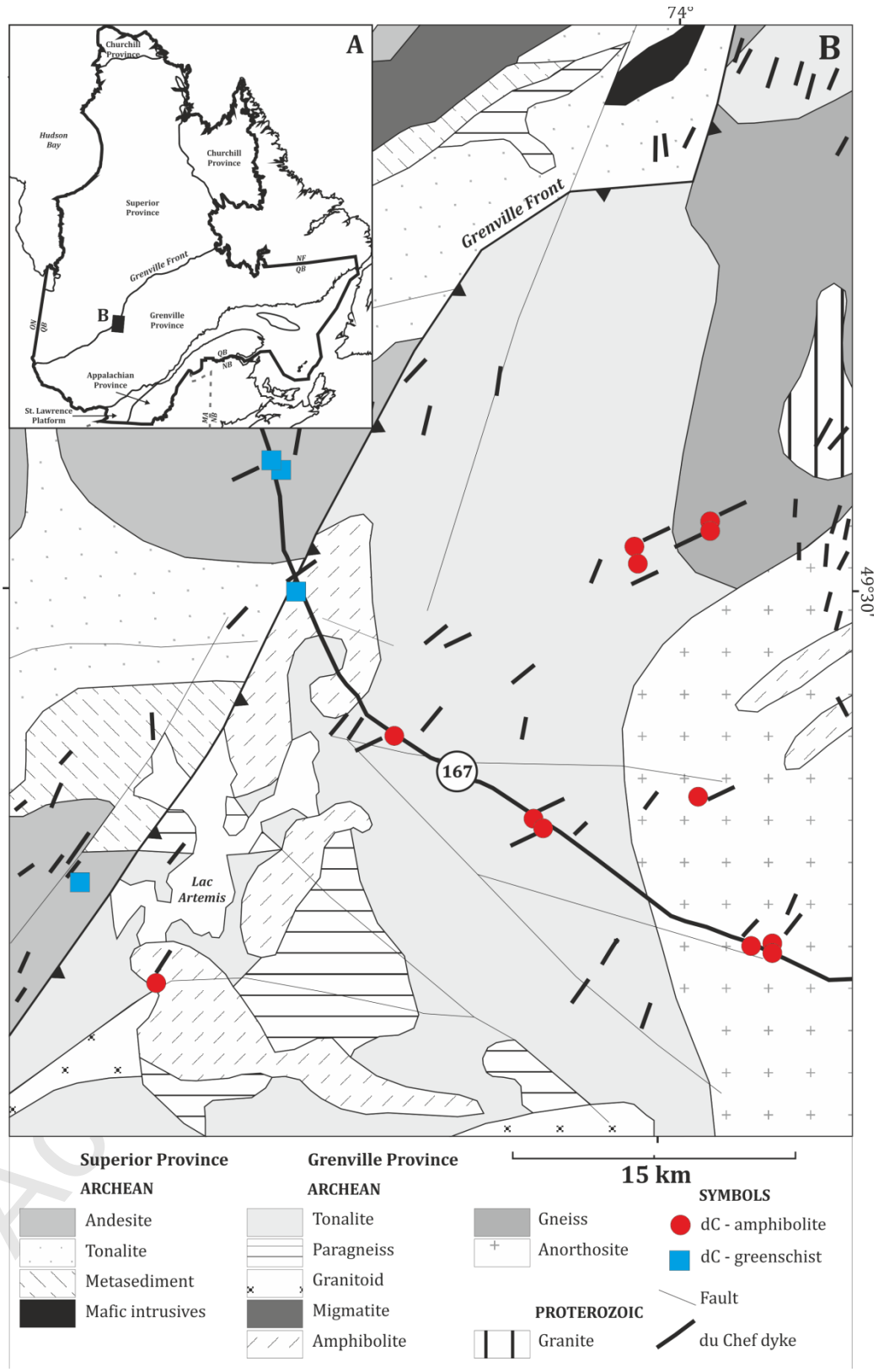

Fig. 1. Geological map of area showing sample locations. Geology modified after Thériault et al. (2012).

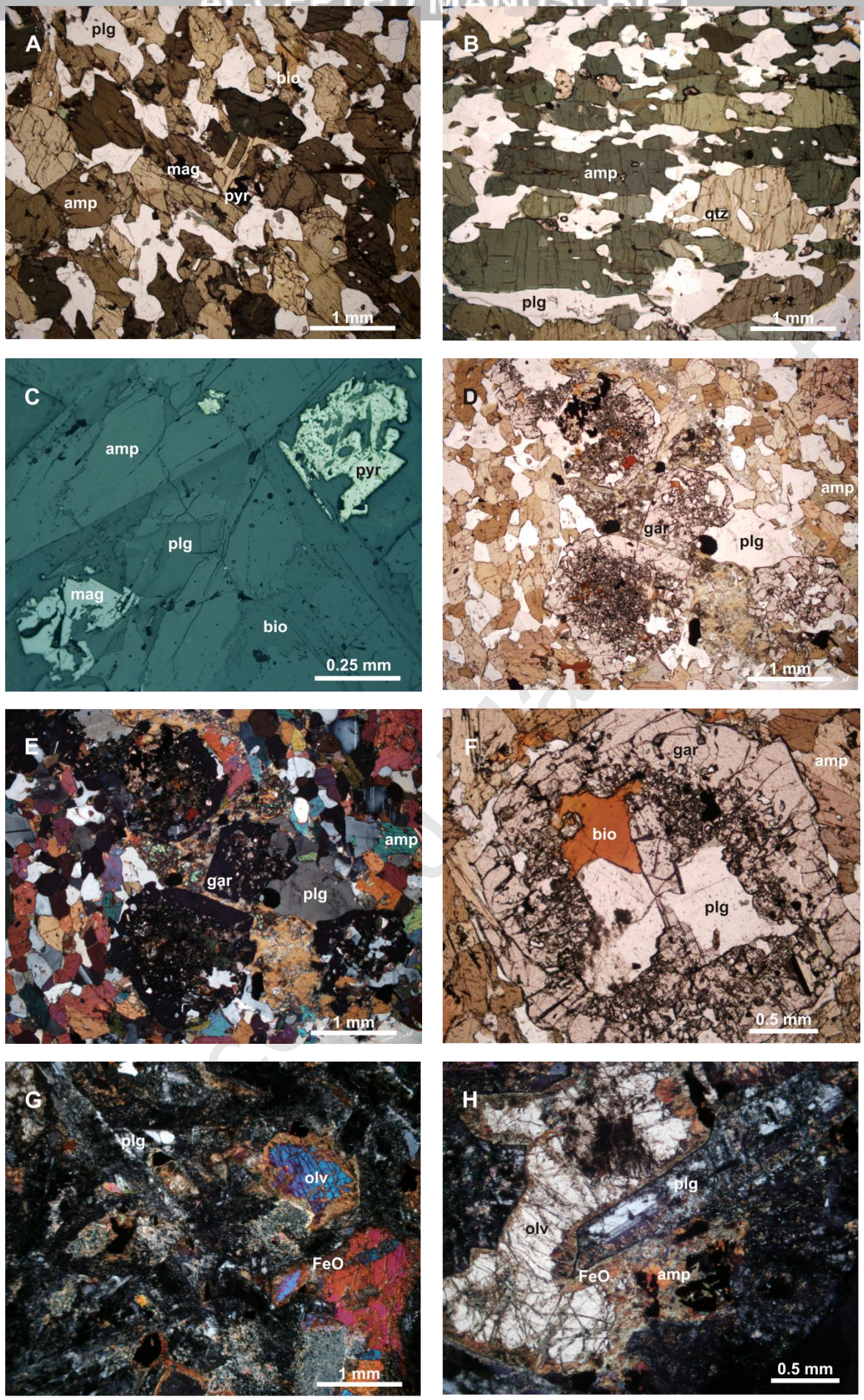

Fig. 2. Photomicrographs of the du Chef dykes: A – general view of non-foliated amphibolite samples; B – general view of foliated amphibolite samples; C – reflected light micrograph showing textures of magnetite and pyrite in amphibolite samples; D – garnet porphyroblasts; E – crosspolarised view of D; F – garnet porphyroblast showing atoll texture; G – general view of non-amphibolitised du Chef dyke; H – alteration of olivine and plagioclase in non-amphibolitised dykes. Abbreviations: amp – amphibole, bio – biotite, plg – plagioclase, mag – magnetite, pyr – pyrite, qtz – quartz, gar – garnet.

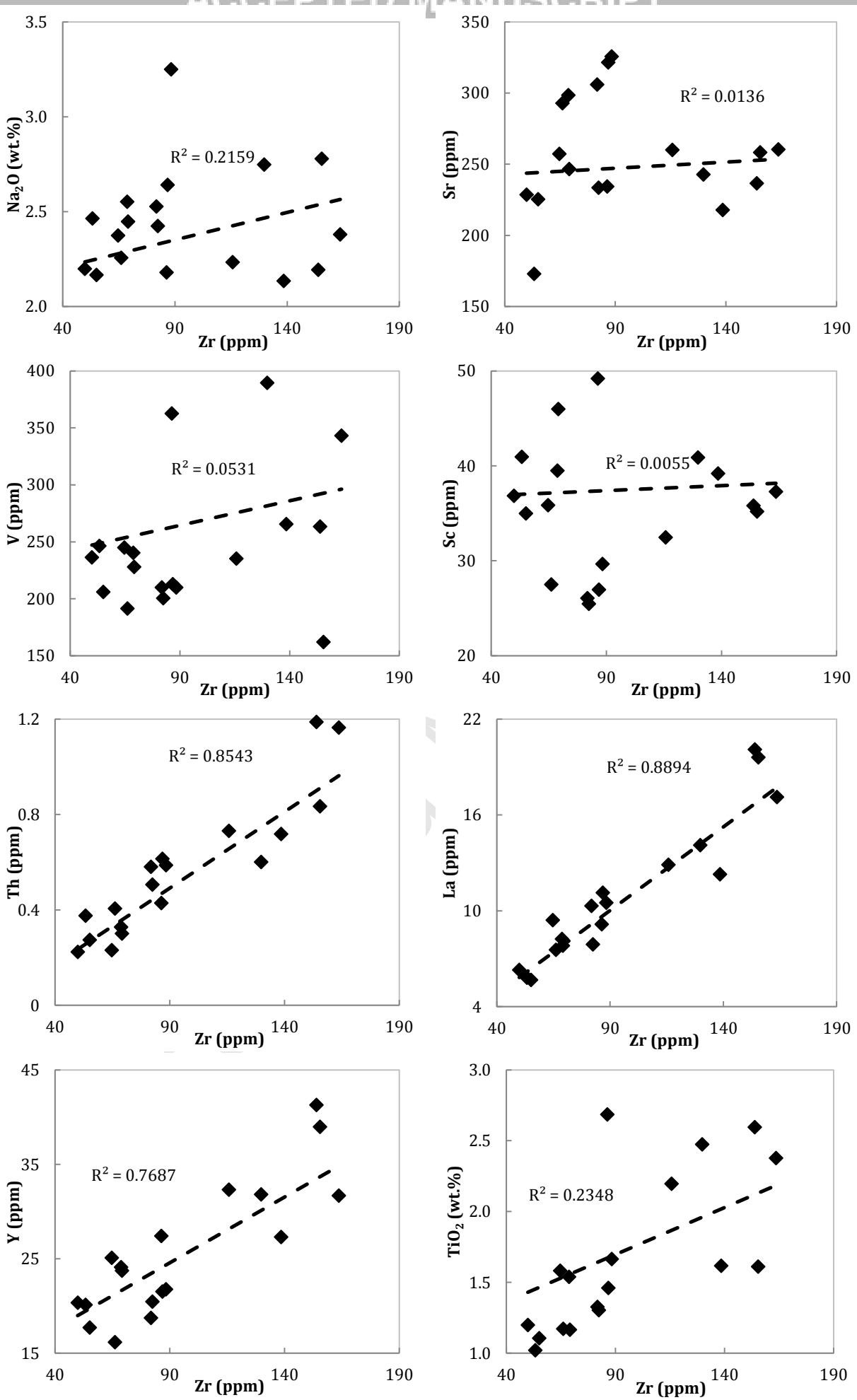

Fig. 3. Bivariate diagrams of selected elements plotted against Zr for the du Chef dykes.

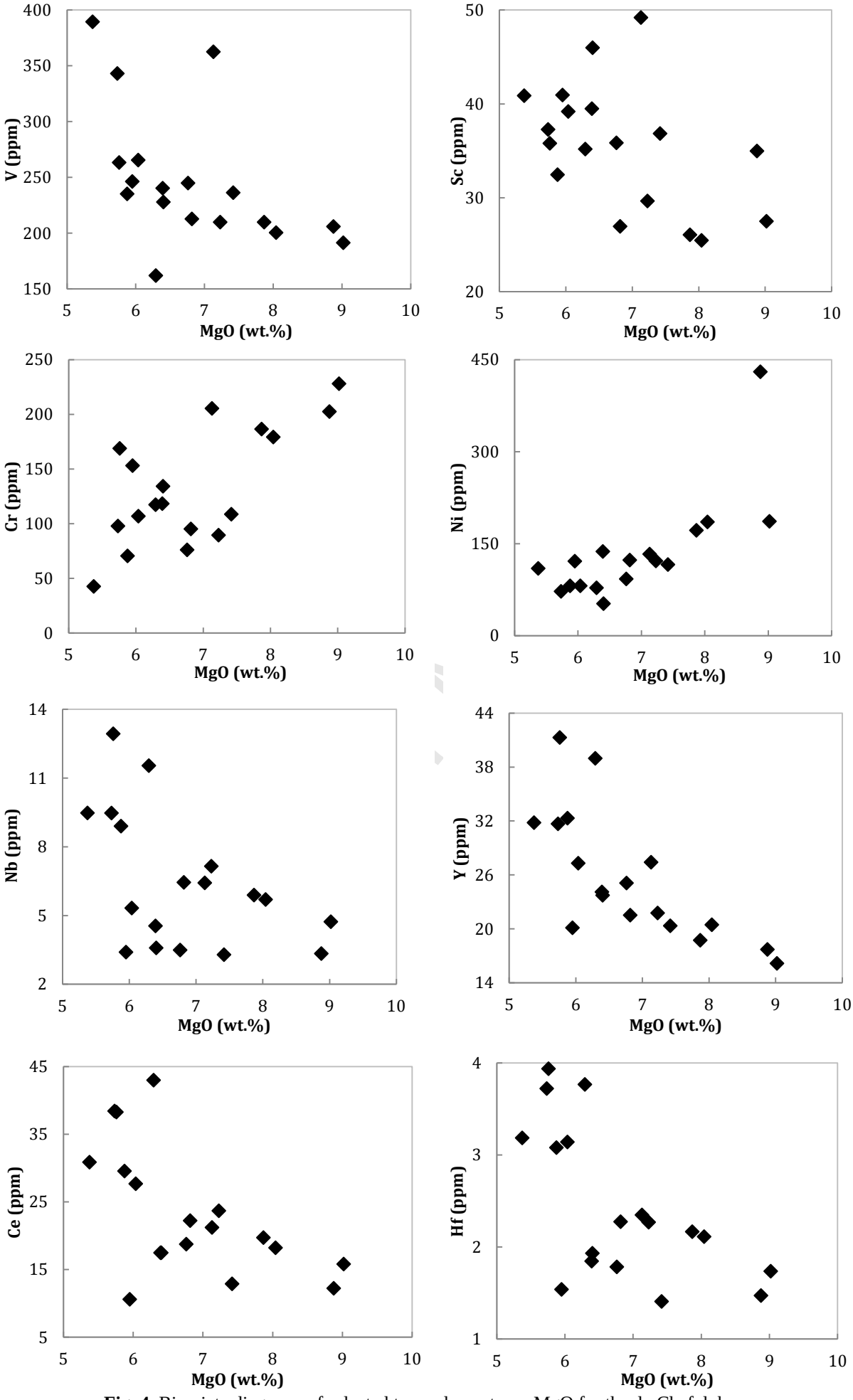

Fig. 4. Bivariate diagrams of selected trace elements vs. MgO for the du Chef dykes.

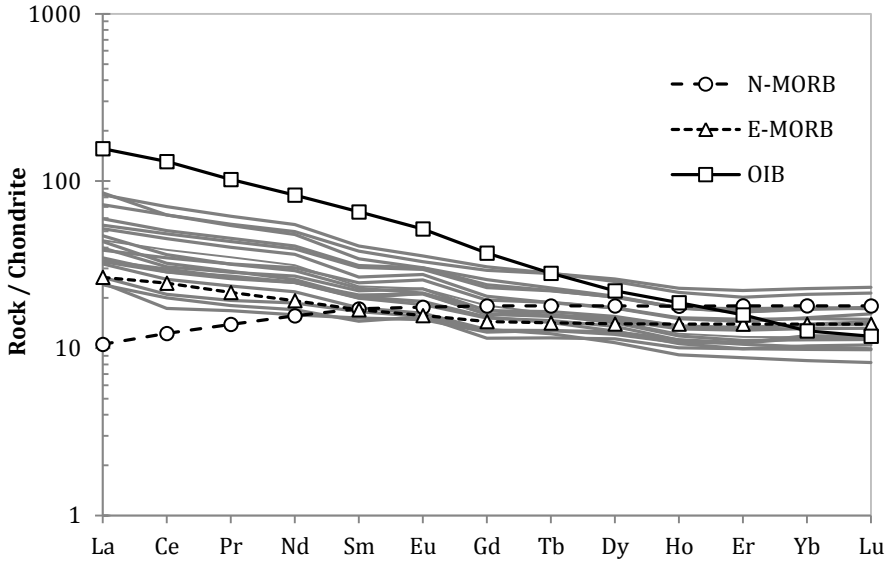

Fig. 5. Chondrite-normalised rare earth element plot of the du Chef dykes. End-members and normalising factors from Sun and McDonough (1989).

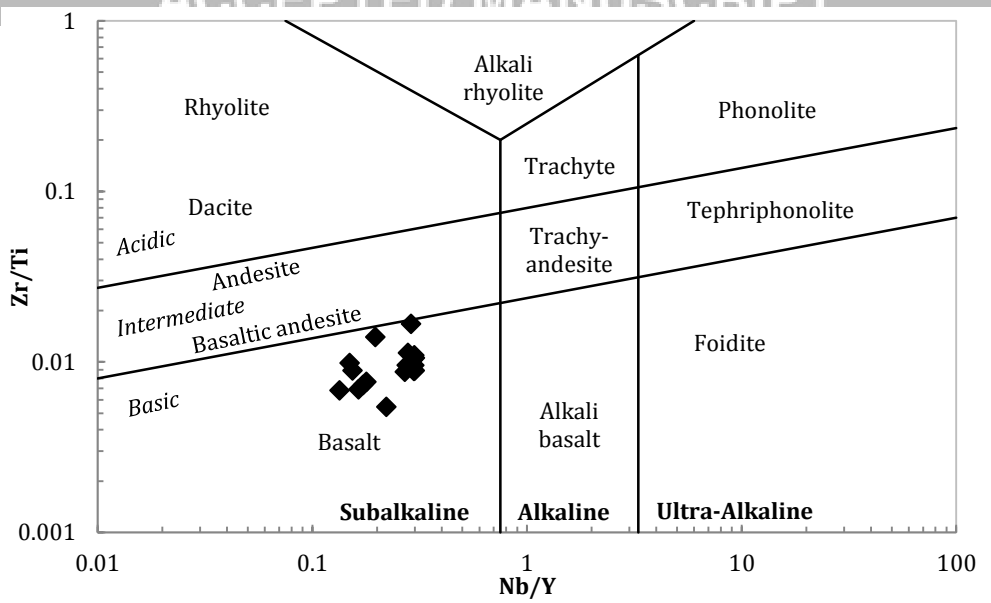

Fig. 6. Zr/Ti vs. Nb/Yb classification diagram (Pearce 1996) for the du Chef dykes.

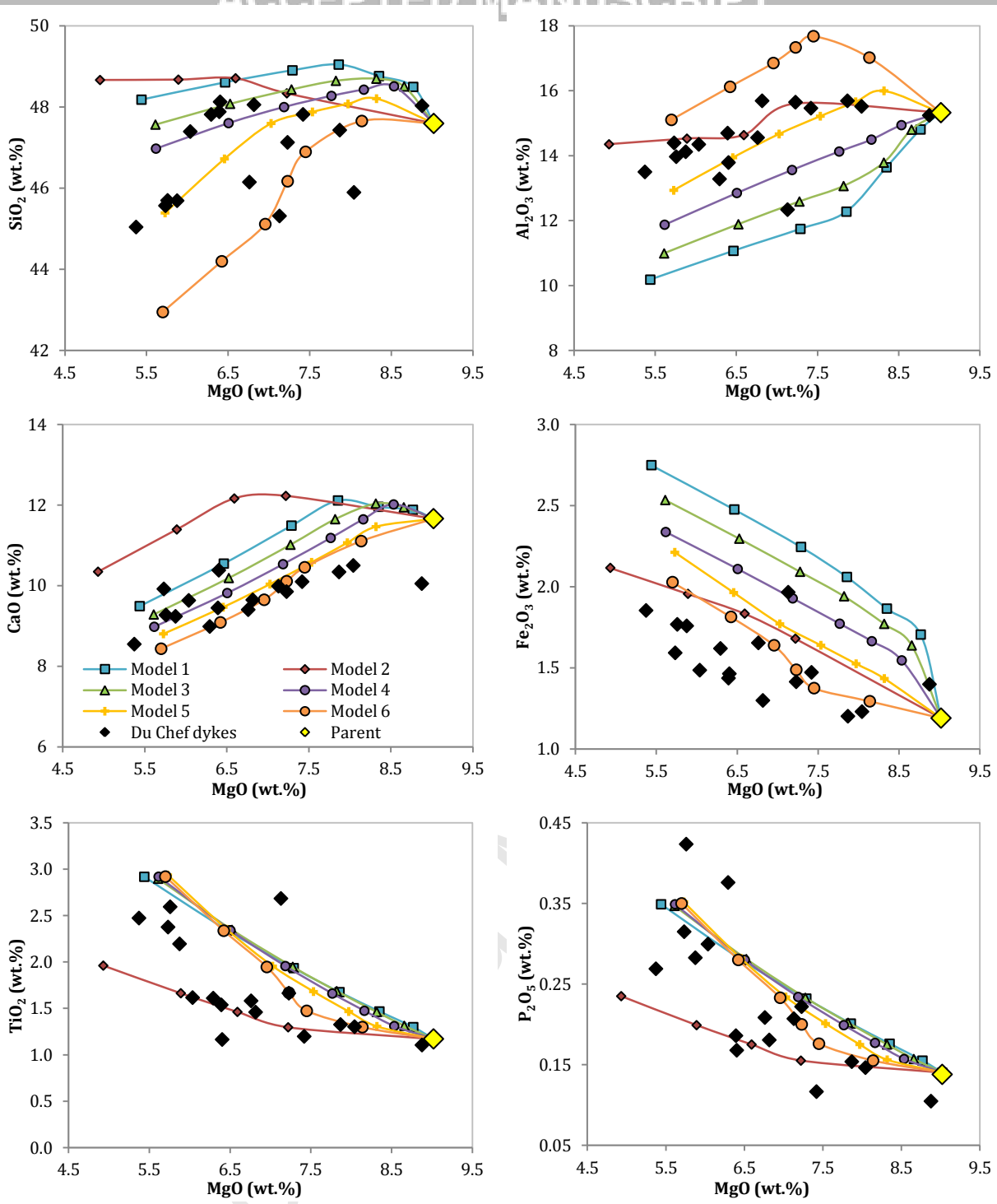

Fig. 7. Bivariate diagrams of selected major elements vs. MgO trends for the du Chef dykes and those predicted by fractional crystallisation of a parent magma with a composition equal to that of sample DC011. Markers on the model lines are placed at intervals of 10% crystallisation.

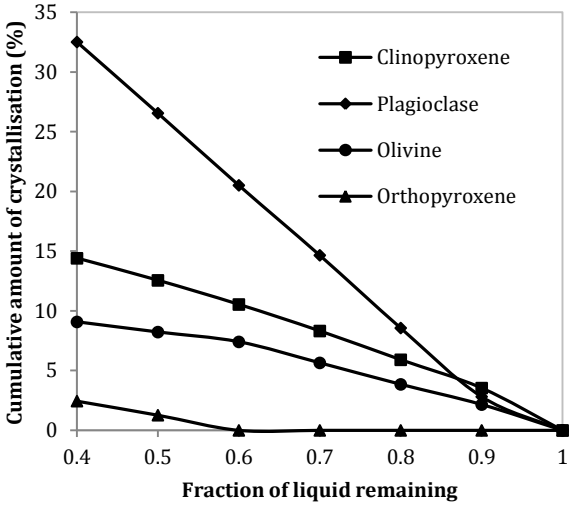

Fig. 8. Diagram showing the cumulative proportions of crystals formed by fractional crystallisation of the du Chef parent at 10% intervals of crystallisation.

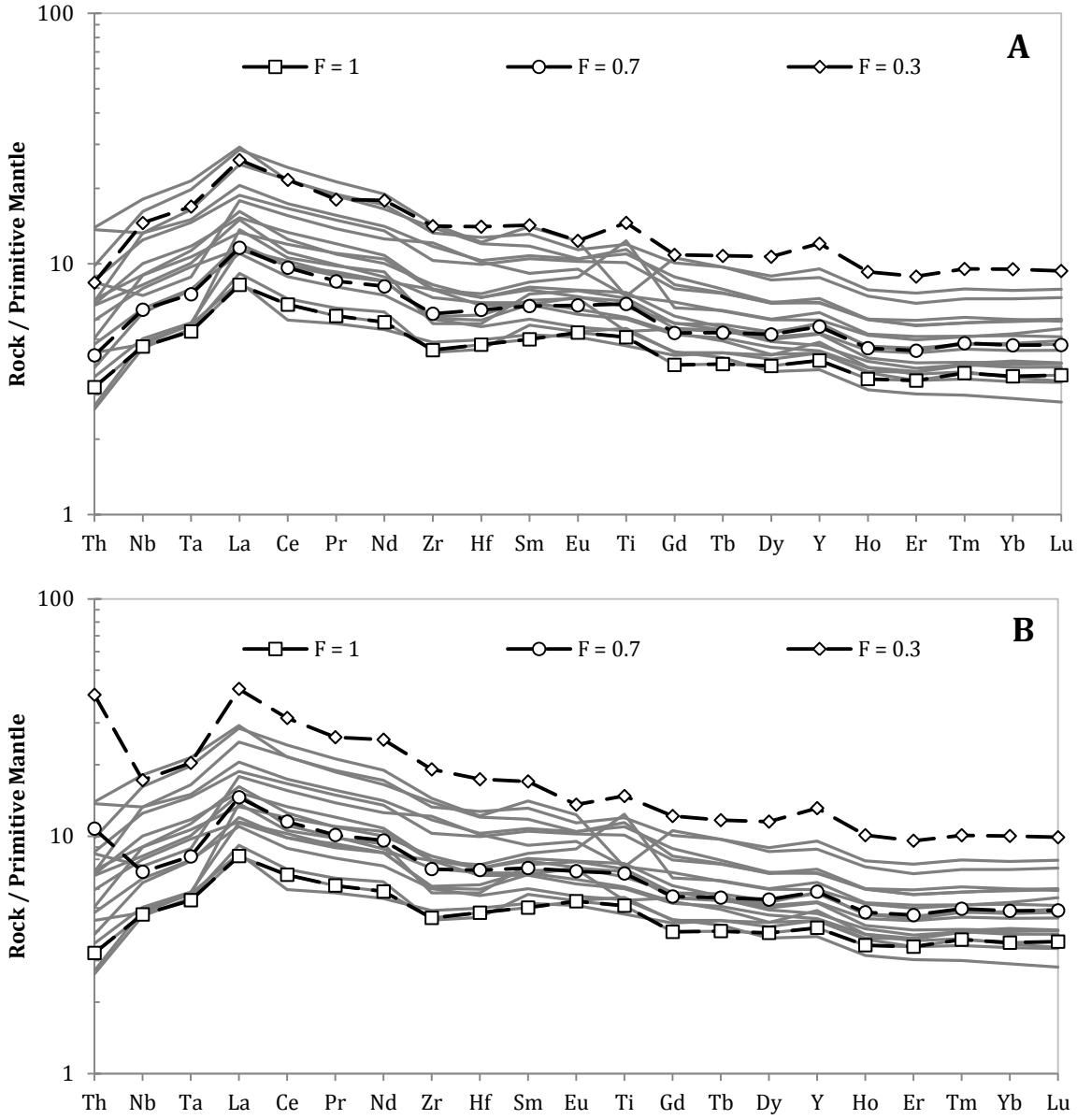

Fig. 9. Primitive mantle-normalised trace element diagrams for the du Chef dykes. Also plotted are the trends predicted by FC (A) and AFC (B) using the starting composition of sample DC011 and the model constraints explained in the text. F = fraction of parent magma remaining as liquid after partial crystallization.

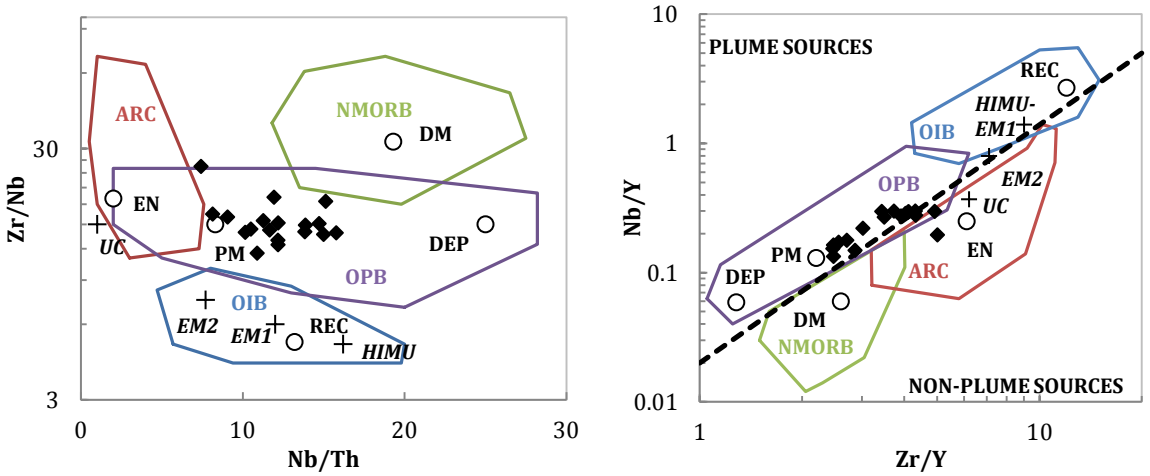

Fig. 10. Zr/Nb vs. Nb/Th diagram (A) and Nb/Y vs. Zr/Y diagram (B) for the du Chef dykes. Field boundaries and end-member compositions from Condie (2005). Abbreviations: PM = Primitive Mantle, DM = shallow depleted mantle, ARC = arc related basalts, NMORB = normal mid-ocean ridge basalt, OPB = oceanic plateau basalt, OIB = oceanic island basalt, DEP = deep depleted mantle, EN = enriched component, REC = recycled component.

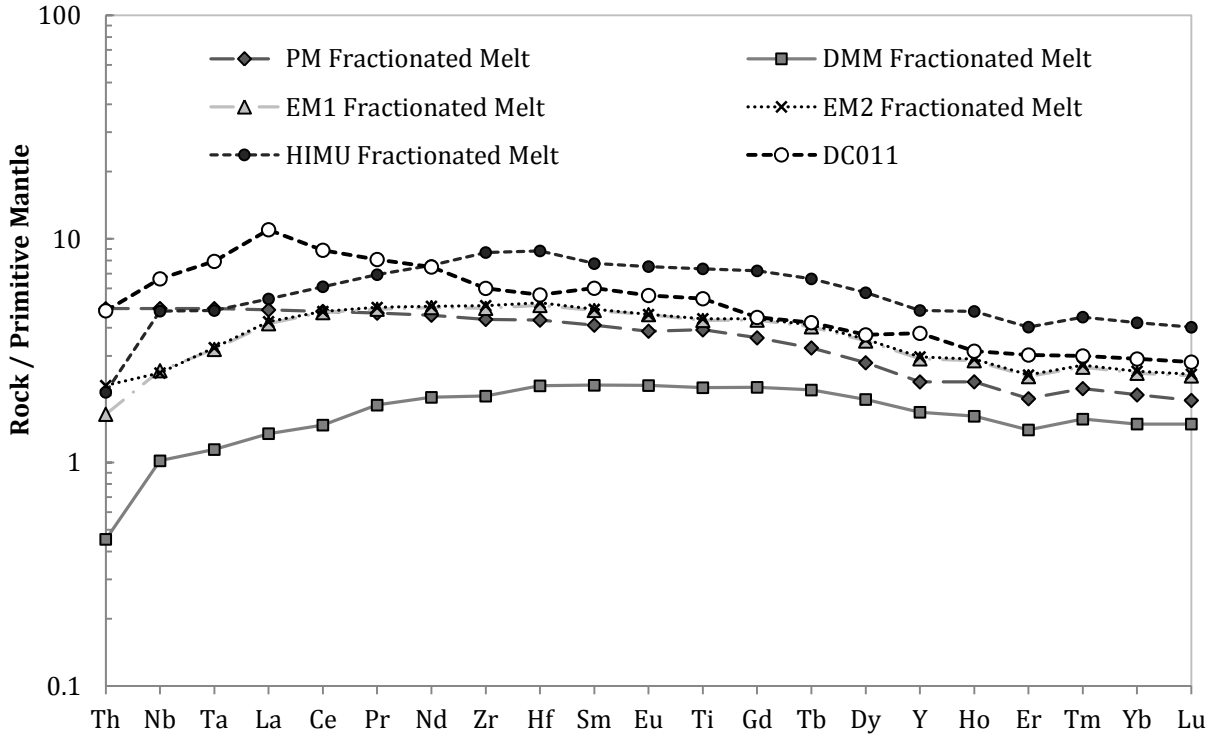

Fig. 11. Primitive mantle-normalised trace element diagrams for the du Chef sample DC011. Also plotted are the trends predicted for magmas which have evolved through 32% fractional crystallisation of olivine, following 30% batch partial melting of garnet lherzolites (Johnston et al. 1990) from the EM1, EM2, DMM, HIMU and PM mantle reservoirs.

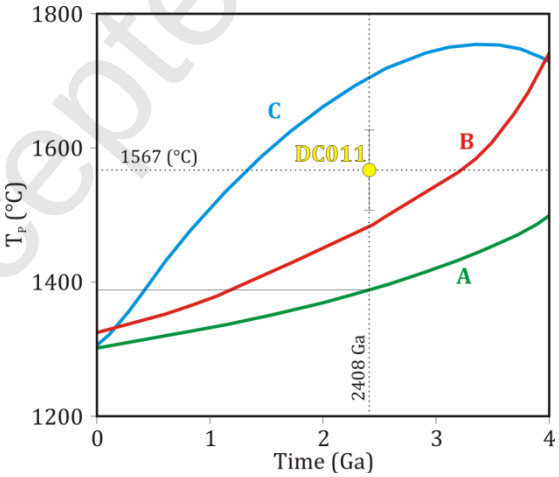

Fig. 12. Temperature evolution of the upper mantle through time using different models; A – Davies (2009); B – Richter (1988); C – Korenaga (2008).

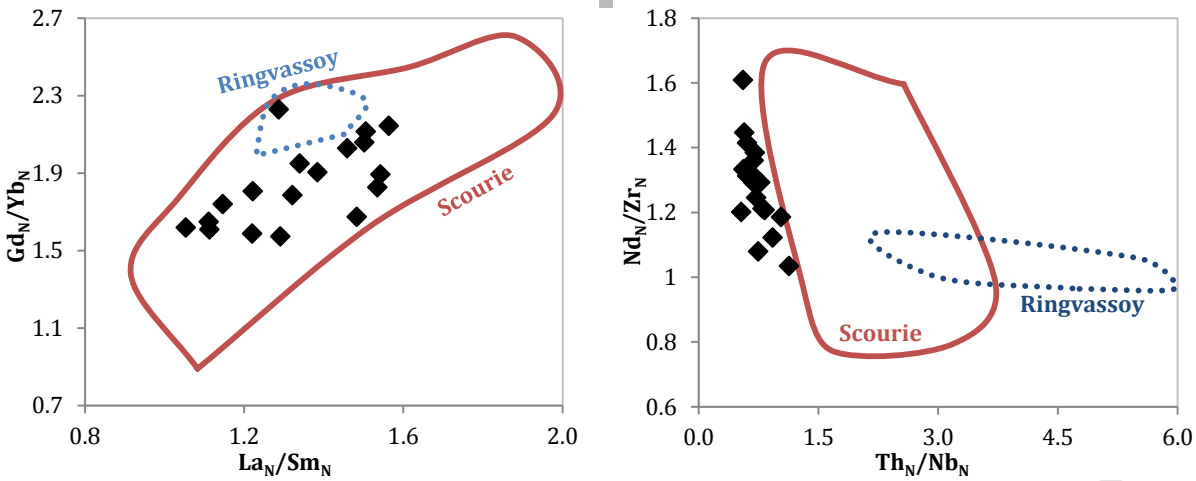

Fig 13. Primitive mantle-normalised bivariate diagrams showing composition of the du Chef dykes, Ringvassoy dykes (Kullerud et al. 2006) and Scourie dykes (Hughes et al. submitted).

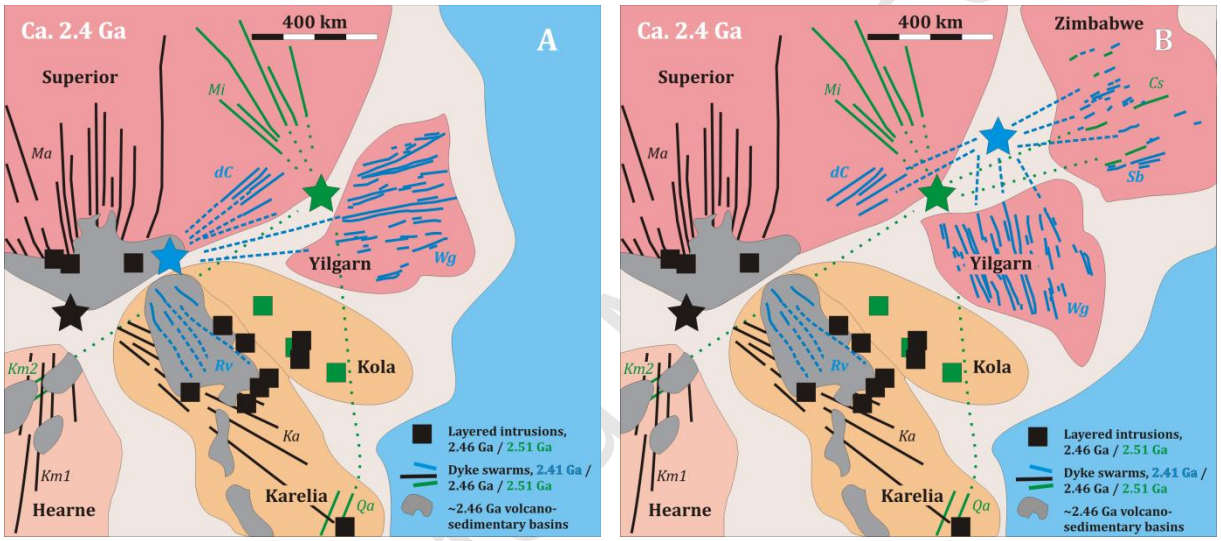

Fig. 14. Ca. 2.4 Ga continental reconstructions showing potential configurations of the eastern margin of Superia. Abbreviations for dyke swarms: Km – Kaminak, Ma – Matachewan, Ka – Karelian, dC – du Chef, Sb – Sebanga, Cs – Crystal Springs, Mi – Mistassini, Qarliit Nunaat, and Rv – Ringvassoy. Modified after Soderlund et al. (2010).